Electrodeposition of Zinc from Acetate Baths

by R Sekar & S. Jayakrishnan*

Zinc electrodeposits are widely used to protect iron and steel from corrosion. Zinc coatings are presently obtained from chloride, sulfate, mixed chloride and sulfate, cyanide and non-cyanide alkaline baths. Atmospheric corrosion is associated with the use of chloride electrolytes. The use of additives, low cathode efficiency and the costly effluent treatment discourage the use of non-cyanide alkaline zinc plating baths. Hence, a better quality zinc plating electrolyte is necessary. In this paper, the authors present a detailed investigation of zinc plating from non-cyanide based acetate electrolytes and the effect of thiamine hydrochloride and gelatin as additives to produce quality bright deposits. The bath and deposit characteristics of acetate-based zinc plating was studied and the results are presented.

It is well known that zinc electrodeposits find wide use in resisting corrosion. They are used on ferrous metals to protect against rust formation. Recently, research has been directed towards the development of non-polluting chemical processes for zinc deposition. Therefore it is of great interest to search for non-toxic electrolytes with good characteristics to replace the pollution-prone baths used in the plating industry. Zinc is relatively low in cost, and the attractive appearance of zinc makes it a popular coating for nuts, bolts, washers, metal stampings and automotive parts. In addition, zinc serves as an effective undercoat for paints. Presently, zinc is electrodeposited from acid baths[1-9] and cyanide baths.[10] Non-cyanide alkaline baths[11-16] have been considered as alternatives to those based on highly toxic cyanide chemistry. Numerous attempts have been made to study different types of acid baths. A review of the literature shows that the electrodeposition of zinc from an acetate bath had not been investigated in detail, except as a minor ingredient in zinc plating baths.[17-19] Therefore, we decided to study the electrodeposition of zinc from acetate-based zinc baths. In this paper, we report on our studies of cathode current efficiency, throwing power, cathodic polarization, microhardness, potentiodynamic polarization, x-ray diffraction and scanning electron microscopy of electrodeposits obtained from acetate-based zinc plating baths under a variety of conditions.

Nuts & Bolts: What This Paper Means to You

Zinc electrodeposits from cyanide baths were once the mainstay in producing this important plated metal. Many non-cyanide substitutes have been developed over the years. The authors describe their work with an acetate-based zinc-plating process, which they say has advantages in obtaining quality bright deposits with improved cathode efficiency and less costly waste treatment.

Experimental

The experiments were carried out in triplicate on mild steel substrates. Surface pretreatment conditions were as follows:

1. Degrease with trichloroethylene
2. Cathodic alkaline clean using the following solution composition and operating conditions:

Sodium hydroxide	35 g/L (4.7 oz/gal)
Sodium carbonate	25 g/L (3.3 oz/gal)
Temperature	70 to 80°C (158 to 176°F)
Duration	2.0 min
Current density	6.0 A/dm^2 (55.7 A/ft^2)
Counter electrode	Stainless steel

3. Water rinse
4. Acid dip (5% H_2SO_4 for 15 sec)
5. Water rinse
6. Distilled water rinse

Cathode current efficiency:

Mechanically polished and cleaned mild steel panels 7.5 × 5 × 0.1 cm (approximately 3 × 2 × 0.04 in.) in size were used as cathodes in an electroplating assembly consisting of two 99.99% pure zinc anodes on either side of the cathode. The three zinc plating baths studied (A, B and C, given in Table 1) were operated at different temperatures and current densities. The cathode current efficiency and plating rate in each case were calculated by weighing the cathodes.

* *Corresponding author:*
Dr. Ramachandran Sekar
Central Electrochemical Research Institute
Karaikudi 630 006
Tamil Nadu, India
E-mail: grsek2004@yahoo.com

Table 1
Composition of the acetate baths studied

Bath	Constituents g/L (oz/gal)		Additives g/L (oz/gal)	
A	Zinc acetate Sodium acetate Aluminum sulfate Boric acid	200 (26.7) 100 (13.4) 30 (4.0) 60 (8.0)	None	
B	Zinc acetate Sodium acetate Aluminum sulfate Boric acid	200 (26.7) 100 (13.4) 30 (4.0) 60 (8.0)	Thiamine-hydrochloride	3.0 (0.4)
C	Zinc acetate Sodium acetate Aluminum sulfate Boric acid	200 (26.7) 100 (13.4) 30 (4.0) 60 (8.0)	Gelatin	3.0 (0.4)

Throwing power:

The assembly used for the studies consisted of a rectangular cell consisting of two cold-rolled steel strips 7.5 × 5 × 0.1 cm (approximately 3 × 2 × 0.04 in.) as cathodes, filling the entire cross-section at both ends and one perforated zinc anode of the same size placed between the cathodes so that its distance from one of the cathodes was one-fifth (1:5) of that from the other. The Field formula was used for calculating the throwing power.

Cathodic polarization (Galvanostatic method)

The pretreated cold rolled steel specimens (6.25 cm^2; ~1.0 in^2) were subject to cathodic polarization studies in each of the zinc plating baths (A, B, C) using a three-electrode cell arrangement. The potential of the steel cathode at different current densities during zinc deposition for the different zinc plating baths were measured vs. SCE and E vs. i curves were plotted.

Microhardness

The hardness of the electrodeposited zinc surface was measured using the static indention method.** A diamond pyramid was pressed into the deposit under a load of 25g for 15 sec and the indentation diagonal measured after the load was removed. The microhardness in kg/mm^2 was determined in each case by using the formula

$$H_v = 1854 \times L/d^2,$$

where L is the applied load in grams, and d is the diagonal of the indentation in micrometers.

** *LECO Microhardness Tester Model M 400, LECO Corporation, St. Joseph, MI 49085-2396.*

*** *JEOL-JSM-35 LF, JEOL USA, Inc., Peabody, MA 01960.*

Potentiodynamic polarization method

The electrodeposited specimens were masked with adhesive tape to expose a 1.0 cm^2 (0.16 in^2) area on one side. A large platinum foil (2.5 × 2.5 cm^2; 1.0 × 1.0 in^2) and saturated calomel electrode were employed as auxilary and reference electrodes respectively, while 5% sodium chloride solution was used as the test solution for zinc.

The polarization behavior was studied in the test electrolyte for zinc deposits of different thicknesses (3, 6, 12, 18 and 24 μm; 118, 236, 472, 708 and 944 μ-in). The working electrode was introduced into the test solution and it was allowed to attain a steady-state potential value. Then the electrode potential was fixed as the open circuit potential. To the open circuit potential (OCP) the steady state polarization was carried out from ±200 mV to the OCP at a scan rate of 1 mV/sec. E_{corr} and i_{corr} values were obtained from the E vs log i curves by the Tafel extrapolation method.

X-ray diffraction

X-ray diffraction patterns were obtained for different zinc deposits obtained from various zinc plating baths at 30°C and 40°C (86°F and 104°F). The deposits produced with and without additives were also studied. The samples were scanned from 30° to 80° (2θ) at a scan rate of 1 degree per minute using CuK_α (λ = 1.5405Å) radiation. The peaks corresponding to the different phases were identified and the corresponding lattice parameters were calculated.

Scanning Electron Microscopy (SEM)

In order to understand the nature of the deposits, the deposits obtained from the three electrolytes were studied visually and by using a scanning electron microscope.*** SEM photographs were taken by using an instrument which possessed an accelerating voltage range of 5 to 35 kV and a magnification range of 10 to 180kX. SEM photographs for the present studies were taken at 25 kV at 1000X magnification. The SEM which makes use of reflected primary electrons and secondary electrons enables one to obtain information from regions which cannot be examined by other techniques. For these tests the plated specimens were cut to 10 × 10 mm (0.4 × 0.4 in) size, suitably mounted, examined and photographed.

Results & discussion

Determination of cathode current efficiency

The cathode current efficiency was determined from different zinc plating electrolytes given in Table 1. The results of the cathode efficiency measurements carried out at different temperatures (30°C, 40°C and 50°C; 86°F, 104°F and 122°F) and current densities (0.5 to 5.0 A/dm^2; 4.6 to 46.4 A/ft^2) in Bath A are presented in Table 2. The time of electrodeposition was varied from 15 min to 1 hr for high and low current densities. The results show that cathode efficiency decreased with increasing current density and temperature. This may have been due to the evolution of hydrogen

Table 2
Influence of current density and temperature on the deposition characteristics of Bath A at pH 5.0

Temperature	Current density, A/dm² (A/ft²)	Cathode efficiency, %	Plating rate, μm/hr (mil/hr)	Deposit quality
30°C (86°F)	0.5 (4.6)	99.36	8.82 (0.35)	Smooth uniform matte white
	1.0 (9.3)	98.80	16.87 (0.66)	
	2.0 (18.6)	97.80	33.30 (1.31)	
	3.0 (27.9)	96.40	50.80 (2.00)	
	4.0 (37.2	95.66	65.84 (2.59)	
	5.0 (46.4)	94.70	81.50 (3.21)	
40°C (104°F)	0.5 (4.6)	99.1	8.80 (0.35)	Smooth uniform matte white
	1.0 (9.3)	97.8	16.69 (0.66)	
	2.0 (18.6)	96.7	33.02 (1.30)	
	3.0 (27.9)	95.3	49.50 (1.95)	
	4.0 (37.2	86.2	58.86 (2.32)	
	5.0 (46.4)	85.3	73.40 (2.89)	
50°C (122°F)	0.5 (4.6)	98.5	8.70 (0.34)	Non-uniform coverage
	1.0 (9.3)	97.9	16.69 (0.66)	Smooth uniform matte white
	2.0 (18.6)	97.4	32.67 (1.29)	Smooth uniform matte white
	3.0 (27.9)	96.9	51.00 (2.01)	Smooth uniform matte white
	4.0 (37.2	96.2	66.20 (2.61)	Smooth uniform matte white
	5.0 (46.4)	91.2	78.50 (3.09)	Smooth uniform matte white

gas at the higher current densities and temperatures. Both poorly covering and smooth uniform matte white deposits were noticed at low and medium current densities, respectively. A powdery deposit was observed at high current densities. It was concluded that the medium current density range of 2.0 to 3.0 A/dm² (18.6 to 27.9 A/ft²) was more conducive to producing a smooth uniform matte white deposit with high cathode efficiency.

The cathode current efficiency was determined for the zinc plat-

Table 3
Influence of current density and temperature on the deposition characteristics of Bath B at pH 5.0

Temperature	Current density, A/dm² (A/ft²)	Cathode efficiency, %	Plating rate, μm/hr (mil/hr)	Deposit quality
30°C (86°F)	0.5 (4.6)	99.4	8.8 (0.35)	Smooth uniform matte white
	1.0 (9.3)	99.3	16.9 (0.66)	Smooth uniform matte white
	2.0 (18.6)	98.1	33.5 (1.32)	Semibright deposit
	3.0 (27.9)	96.6	49.5 (1.95)	Bright
	4.0 (37.2	94.5	64.3 (2.53)	Bright
	5.0 (46.4)	94.1	80.6 (3.17)	Bright
40°C (104°F)	0.5 (4.6)	99.8	8.9 (0.35)	Light grey
	1.0 (9.3)	98.9	16.7 (0.66)	Light grey
	2.0 (18.6)	97.2	33.3 (1.31)	Semibright
	3.0 (27.9)	96.9	49.6 (1.95)	Semibright
	4.0 (37.2	96.6	66.0 (2.60)	Semibright
	5.0 (46.4)	95.0	81.1 (3.19)	Semibright
50°C (122°F)	0.5 (4.6)	99.9	8.9 (0.35)	Light grey
	1.0 (9.3)	98.1	16.6 (0.65)	Light grey
	2.0 (18.6)	96.7	29.5 (1.16)	Light grey
	3.0 (27.9)	87.4	45.4 (1.79)	Light grey
	4.0 (37.2	86.4	50.0 (1.97)	Dark grey
	5.0 (46.4)	73.2	62.6 (2.46)	Dark grey

Table 4
Influence of current density and temperature on the deposition characteristics of Bath C at pH 5.0

Temperature	Current density, A/dm² (A/ft²)	Cathode efficiency, %	Plating rate, μm/hr (mil/hr)	Deposit quality
30°C (86°F)	0.5 (4.6)	99.9	8.9 (0.35)	Smooth uniform matte white
	1.0 (9.3)	99.5	17.0 (0.67)	Smooth uniform matte white
	2.0 (18.6)	93.4	31.9 (1.26)	Smooth uniform matte white
	3.0 (27.9)	91.9	47.1 (1.85)	Bright
	4.0 (37.2	89.5	61.1 (2.40)	Bright
	5.0 (46.4)	84.1	71.8 (2.83)	Bright
40°C (104°F)	0.5 (4.6)	97.6	8.7 (0.34)	Light grey
	1.0 (9.3)	97.6	16.7 (0.66)	Light grey
	2.0 (18.6)	92.9	31.7 (1.25)	Light grey
	3.0 (27.9)	90.7	46.5 (1.83)	Semibright
	4.0 (37.2	86.8	59.3 (2.33)	Semibright
	5.0 (46.4)	81.9	70.0 (2.76)	Semibright
50°C (122°F)	0.5 (4.6)	96.4	8.6 (0.34)	Light grey
	1.0 (9.3)	97.0	16.8 (0.66)	Light grey
	2.0 (18.6)	87.9	30.0 (1.18)	Light grey
	3.0 (27.9)	89.0	45.6 (1.80)	Dark grey
	4.0 (37.2	85.3	58.3 (2.30)	Dark grey
	5.0 (46.4)	79.4	67.8 (2.67)	Dark grey

ing bath with the addition of 3.0 g/L (0.4 oz/gal) thiamine hydrochloride (Bath B) at various temperatures and current densities and the results are presented in Table 3. In general, the cathode efficiency decreased with increasing temperature and current density. This again may have been due to hydrogen evolution occurring at the higher current densities and temperatures. Bright deposits were observed at and above 2.5 A/dm² (23.2 A/ft²), while matte white to light grey deposits were obtained at low current densities. When the bath was operated at 40°C or 50°C (104°F or 122°F), the deposit became powdery and dark grey.

The results of current efficiency studies from Bath C containing 3.0 g/L (0.4 oz/gal) of gelatin as an additive at various temperatures and current densities are presented in Table 4. The results show that the cathode efficiency gradually decreased with increasing current density and temperature as noted in the previous cases.

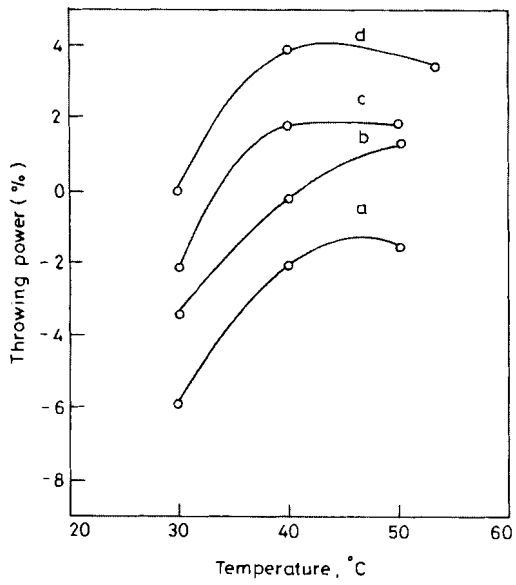

Figure 1—Effect of temperature and current density on throwing power for Bath A: (a) 1.0 A/dm² (9.3 A/ft²); (b) 2.0 A/dm² (18.6 A/ft²); (c) 3.0 A/dm² (27.9 A/ft²); (d) 4.0 A/dm² (37.2 A/ft²).

Determination of throwing power

In general, throwing power increases with temperature, current density, metal ion concentration and agitation.[20] Figure 1 presents the variation of throwing power at different current densities and temperatures. When temperature and current density increased, the throwing power of the bath clearly increased. This could be attributed to an increase in cathodic polarization with increasing temperature and current density.

Figure 2 presents the variation of throwing power with different current densities and temperatures in Bath B with 3.0 g/L (0.4 oz/gal) thiamine hydrochloride added. Initially, the throwing power decreased with increasing temperature and thereafter increased with temperature. The throwing power was greater at lower current densities and higher temperatures. In general, throwing power was high at low current densities. We concluded that the throwing power in Bath B increased with temperature and decreased with increasing current density.

Figure 3 presents the variation of throwing power at different current densities and temperatures in Bath C, containing 3.0 g/L (0.4 oz/gal) gelatin. The throwing power decreased with increasing current density and increased with increasing temperature, especially at high current densities. Thus the throwing power increased with increasing temperature from 1.0 to 2.0 A/dm² (9.3 to 18.6 A/ft²). In the range from 3.0 to 4.0 A/dm² (27.9 to 37.2 A/ft²), throw-

ing power decreased rapidly with increasing temperature, even reaching negative values.

Cathodic polarization (Galvanostatic method)

The potential of steel cathodes at different current densities during zinc deposition from the three baths was measured and is shown in Fig. 4. The potential in Bath C exhibited more negative values at all current densities when compared to Baths A and B. In general, the increase in current density corresponded to increases in polarization. In both the thiamine hydrochloride bath (B) and gelatin bath (C), the cathode potential shifted to more negative values when compared with the additive-free bath. From these studies we concluded that the electrolytes containing thiamine hydrochloride and gelatin polarized the cathode surface to a greater extent. The higher the polarization, the stronger was the adsorption on the active sites of the cathode surface.[21,22]

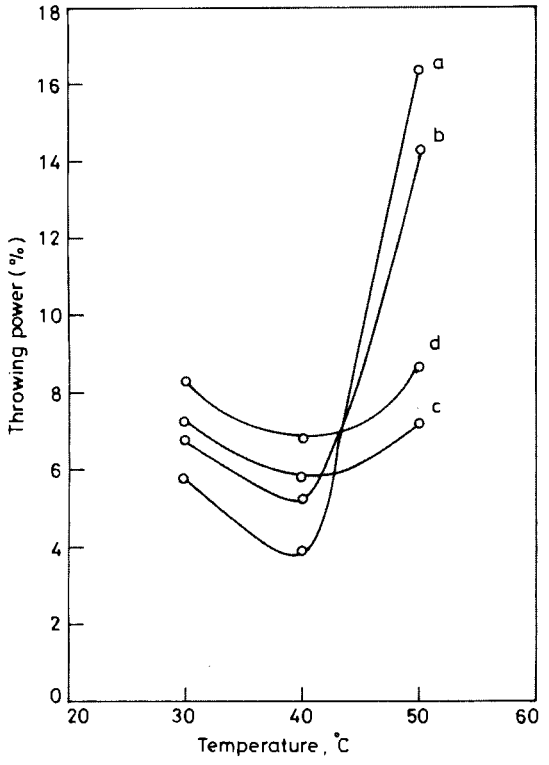

Figure 2—Effect of temperature and current density on throwing power for Bath B: (a) 1.0 A/dm² (9.3 A/ft²); (b) 2.0 A/dm² (18.6 A/ft²); (c) 3.0 A/dm² (27.9 A/ft²); (d) 4.0 A/dm² (37.2 A/ft²).

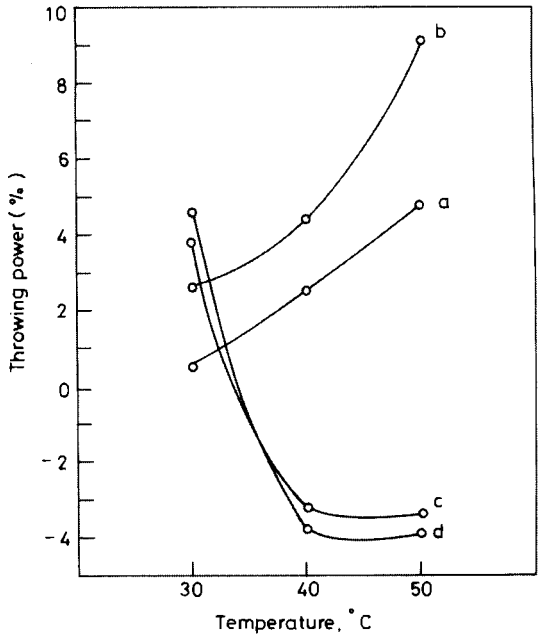

Figure 3—Effect of temperature and current density on throwing power for Bath C: (a) 1.0 A/dm² (9.3 A/ft²); (b) 2.0 A/dm² (18.6 A/ft²); (c) 3.0 A/dm² (27.9 A/ft²); (d) 4.0 A/dm² (37.2 A/ft²).

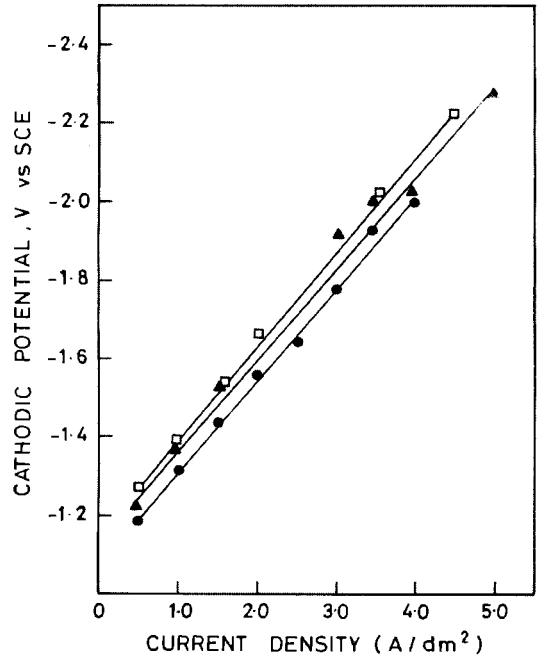

Figure 4—Cathodic polarization curves during zinc deposition in different baths at different current densities at 30°C (86°F) and pH 5.0: Bath A, ●; Bath B, ▲; Bath C, ❑.

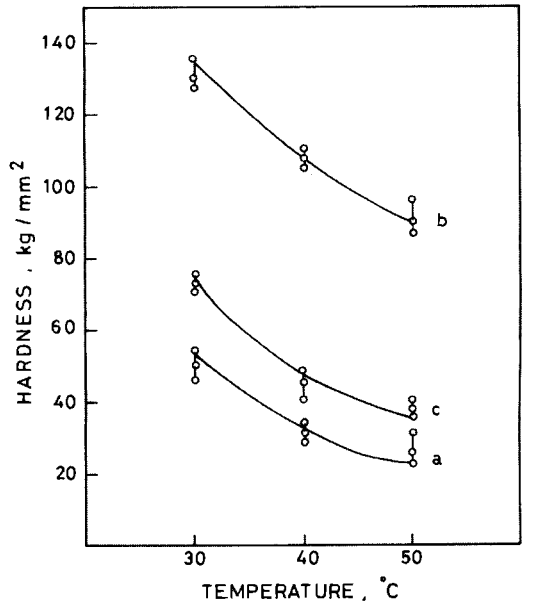

Figure 5—Microhardness of zinc deposits obtained from different zinc plating baths at different temperatures: (a) Bath A, (b) Bath B, (c) Bath C.

Microhardness

Figure 5 shows the variation in microhardness of the zinc deposits with solution temperature. Additive-free Bath A exhibited a reasonable value of microhardness. The hardness value of deposits obtained at 40°C and 50°C (104°F and 122°F) were low. In general, sulfate ions decreased the hardness of the electrodeposits but amino-, thio- or nitro- compounds increased the hardness of the electrodeposits.[3]

The curve "b" in Fig. 5 shows that by the addition of thiamine hydrochloride (Bath B), high-hardness deposits could be obtained at 30°C (86°F). The hardness values obtained at 40°C and 50°C (104°F and 122°F) were low. These results clearly show that amino- and thio- groups improved the hardness of the electrodeposits. At high temperatures the additive may decompose or form a complex which results in the decreased hardness. The curve "c" in Fig. 5 shows that the presence of gelatin as additive (Bath C) produced deposits with reasonably high hardness values at 30°C (86°F). At 40°C and 50°C (104°F and 122°F) the hardness decreased. This may be related to the decomposition of gelatin at high temperatures. Higher hardness values were noted for the deposits obtained from thiamine hydrochloride baths, when compared to the gelatin-containing baths.

Potentiodynamic polarization studies

Anodic and cathodic polarization experiments were carried out on zinc-plated mild steel samples up to ±200 mV from the open circuit potential at a sweep rate of 1.0 mV/sec. From the polarization curves, corrosion current densities could be obtained by extrapolating the linear segments of the anodic and cathodic curves. The parameters derived from E vs. log i curves for different zinc deposits of varying thicknesses in 5% NaCl solution at 1 mV/sec and at 30°C (86°F) are given in Table 5.

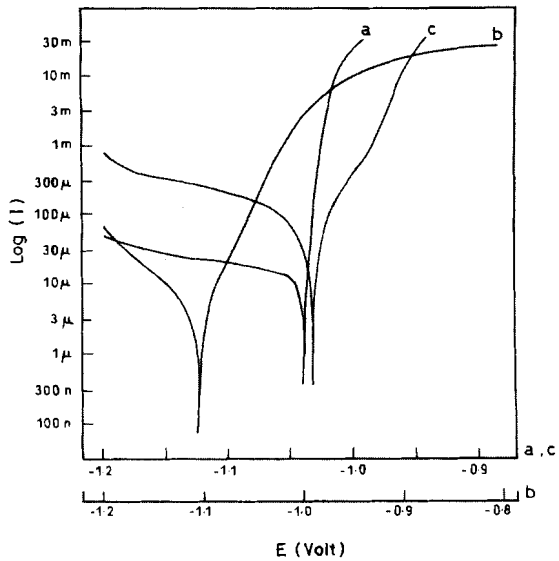

Figure 6—Typical potentiodynamic polarization curves for 3-µm (118-µ-in) zinc deposits obtained from different baths in 5% NaCl solution: (a) Bath A, (b) Bath B, (c) Bath C.

Figure 6 presents the typical potentiodynamic polarization curves obtained for 3-µm (118-µ-in) thick deposits from Baths A, B and C. Baths B and C exhibited more noble values when compared to Bath A. The corrosion current density was also low in both Baths B and C as compared with Bath A, presumably due to the effect of the additives.

Figure 7 shows typical potentiodynamic polarization curves for deposits obtained from Baths A, B and C for a 6-µm (236-µ-in) thickness. There was no significant change of corrosion potential in all deposits, but Baths B and C exhibited a lower corrosion current when compared with Bath A.

Table 5
Parameters derived from E-log I curves for zinc deposits of different thicknesses obtained in 5% NaCl solution at 1 mV/sec at 30°C (86°F)

Deposit from bath	Thickness (µm)	Corrosion current (µA/cm²)	Corrosion potential (mV_{SCE})	Tafel slopes (mV/decade)		Figure No.
				Anodic	Cathodic	
A	3	7.50	-1013	23	32	
B	3	4.75	-1027	29	52	6
C	3	6.60	-1008	26	52	
A	6	6.78	-1020	19	32	
B	6	4.27	-1029	19	39	7
C	6	5.80	-1018	29	52	
A	12	6.20	-1038	19	65	
B	12	3.98	-1020	26	58	8
C	12	5.20	-1025	23	65	
A	18	5.60	-1040	23	35	
B	18	3.20	-1038	29	65	9
C	18	4.90	-1032	23	45	
A	24	5.50	-1042	26	55	
B	24	3.20	-1042	23	52	10
C	24	4.86	-1070	35	42	

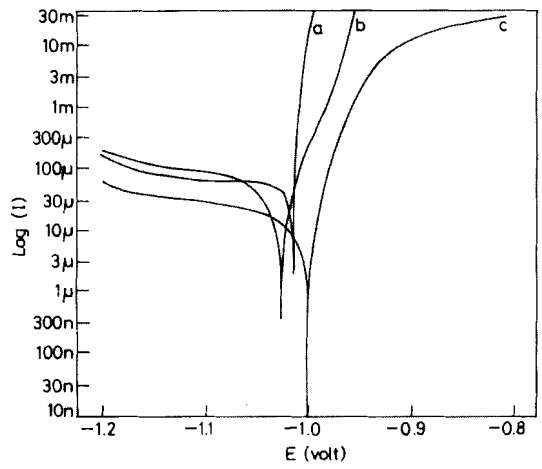

Figure 7—Typical potentiodynamic polarization curves for 6-μm (236-μ-in) zinc deposits obtained from different baths in 5% NaCl solution: (a) Bath A, (b) Bath B, (c) Bath C.

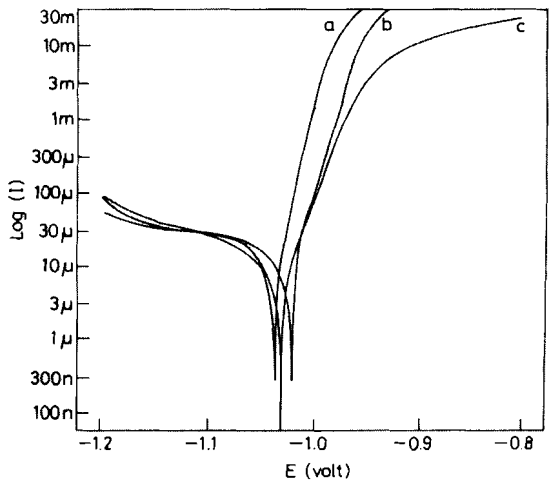

Figure 8—Typical potentiodynamic polarization curves for 12-μm (472-μ-in) zinc deposits obtained from different baths in 5% NaCl solution: (a) Bath A, (b) Bath B, (c) Bath C.

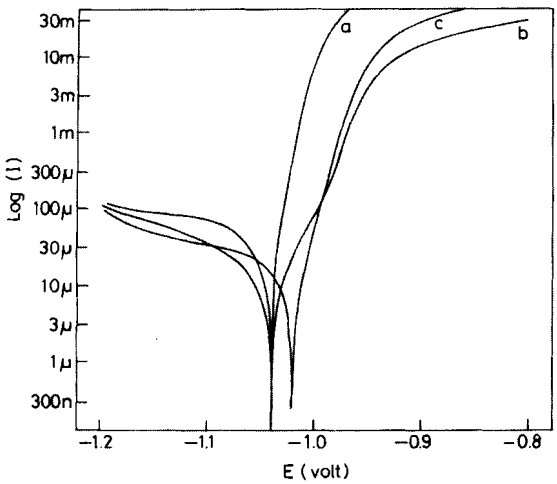

Figure 9—Typical potentiodynamic polarization curves for 18-μm (709-μ-in) zinc deposits obtained from different baths in 5% NaCl solution: (a) Bath A, (b) Bath B, (c) Bath C.

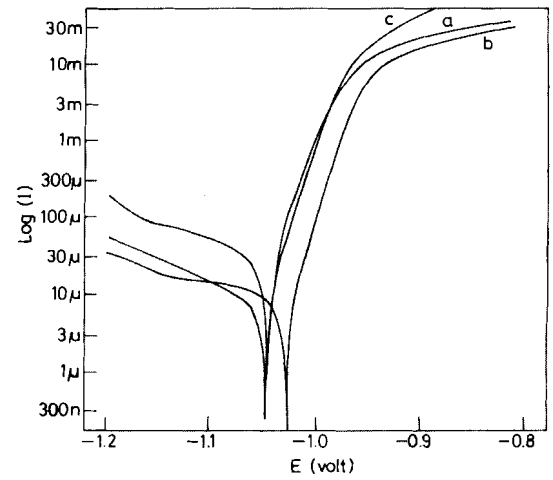

Figure 10—Typical potentiodynamic polarization curves for 24-μm (944-μ-in) zinc deposits obtained from different baths in 5% NaCl solution: (a) Bath A, (b) Bath B, (c) Bath C.

Figures 8, 9 and 10 show the typical potentiodynamic polarization curves for deposits obtained from baths A, B and C for 12-, 18- and 24-μm (472-, 709- and 945-μ-in) thick deposits, respectively. There was no remarkable change in corrosion current with zinc deposits versus thickness obtained from Baths A, B and C, although Baths B and C exhibited a slightly lower corrosion current under all conditions studied. From these studies we concluded that both thiamine hydrochloride and gelatin will retard the dissolution of zinc. These additives improved the grain size and any porosity was completely filled.[23,24] In general, for industrial applications, a 12-μm (472-μ-in) thick zinc deposit is more suitable for good corrosion protection.

X-Ray diffraction

X-ray diffractograms obtained for the zinc electrodeposited from Bath A) are shown in Fig. 11. All deposits were seen to be polycrystalline and assumed a simple hexagonal structure. The reflection of the (103) plane was predominant. A c/a ratio of 1.8554 was obtained and was in good agreement with the reported standard. The "d" values are presented in Tables 6 and 7 at 30°C and 40°C (86°F and 104°F), respectively. No peaks other than those of zinc were observed. It was observed in Fig. 11 that the (100) reflection plane was predominant for the deposit obtained after the addition of thiamine hydrochloride (Bath B) or gelatin (Bath C).

When the bath temperature was raised to 40°C (104°F), the preferred orientation was along the (101) plane for all three baths, as shown in Fig.12. The reduction in peak intensities along the (102), (103) and (112) planes was observed when the additives were added. Tables 6 and 7 show that the observed "d" value was in good agreement with standard values for zinc deposition (JCPDS file No. 1* 40831 Zn).

Scanning electron microscopy

Deposit from Bath A, additive-free. In order to determine the surface structure of the deposit, SEM studies were undertaken. During deposition, the layering, grain size and direction of crystalline growth depend on the cathodic overvoltage and inhibition conditions involved. Figure 13 shows the SEM photos obtained for

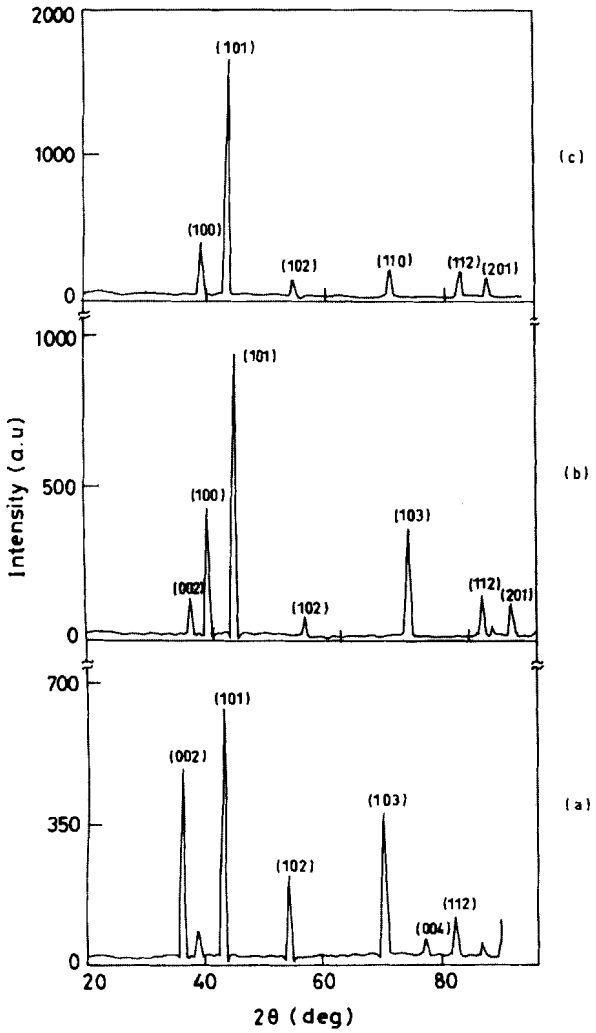

Figure 11—Typical XRD patterns for zinc deposits obtained at 30°C (86°F) from: (a) Bath A, (b) Bath B, (c) Bath C.

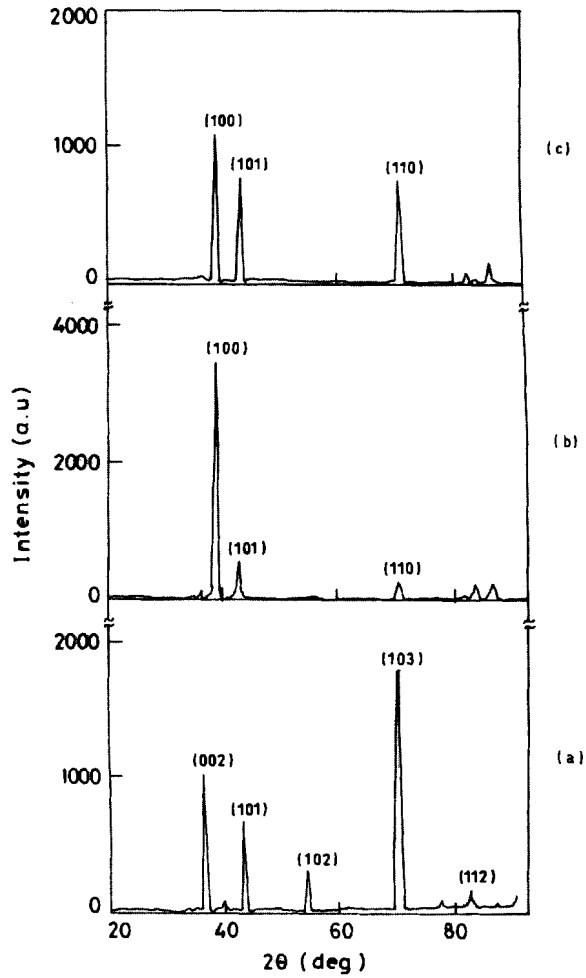

Figure 12—Typical XRD patterns for zinc deposits obtained at 40°C (104°F) from: (a) Bath A, (b) Bath B, (c) Bath C.

Table 6
X-ray diffraction data for electrodeposited zinc obtained at 30°C (86°F)

Bath	'd' observed	'd' standard	hkl	Lattice parameters (nm)		c/a ratio	Structure
				a	c		
A	2.466 2.083 1.682 1.338 1.171	2.473 2.091 1.687 1.342 1.172	002 101 102 103 112	2.6585	4.9326	1.8554	Hexagonal
B	2.325 2.102	2.308 2.091	100 101	2.6850	4.9147	1.8304	Hexagonal
C	2.302 2.088 1.331 1.122	2.308 2.091 1.332 1.123	100 101 110 201	2.6578	4.9629	1.8672	Hexagonal

the three baths studied. The lateral growth of the nuclei gave rise to relatively large crystallites, as seen in Fig. 13(a).[25,26] A slightly improved crystallinity could be observed in Fig. 13(b) for the deposit obtained at 40°C (104°F).

Deposit from Bath B, containing thiamine hydrochloride. Figure 13(c) shows that the addition of 3 g/L (0.4 oz/gal) thiamine hydrochloride to the plating bath promoted a fine grained structure. Fig. 13(d) shows that an improved grain size covering the entire area could be produced at 40°C 104°F).

Deposit from Bath C, containing gelatin. Figure 13(e) shows the results of adding 3 g/L (0.4 oz/gal) of gelatin to the zinc bath at 30°C (86°F). A small platelet structure can be seen. The surface morphology of the deposit obtained at 40°C (104°F), in Fig. 13(f), showed a fiber-like structure with a reduction of platelet size.

Conclusions

From the studies carried out it may be concluded that bright deposits with good values of throwing power, cathode current efficiency and microhardness can be obtained from zinc acetate electrolytes with the addition of thiamine hydrochloride. It may also be further noted that thiamine hydrochloride and gelatin-containing baths polarize the cathode surface to a greater extent. Potentiodynamic polarization studies reveal that thiamine hydrochloride and gelatin will retard the dissolution of zinc. These additives will improve the grain size and porosity is completely filled. XRD studies show that

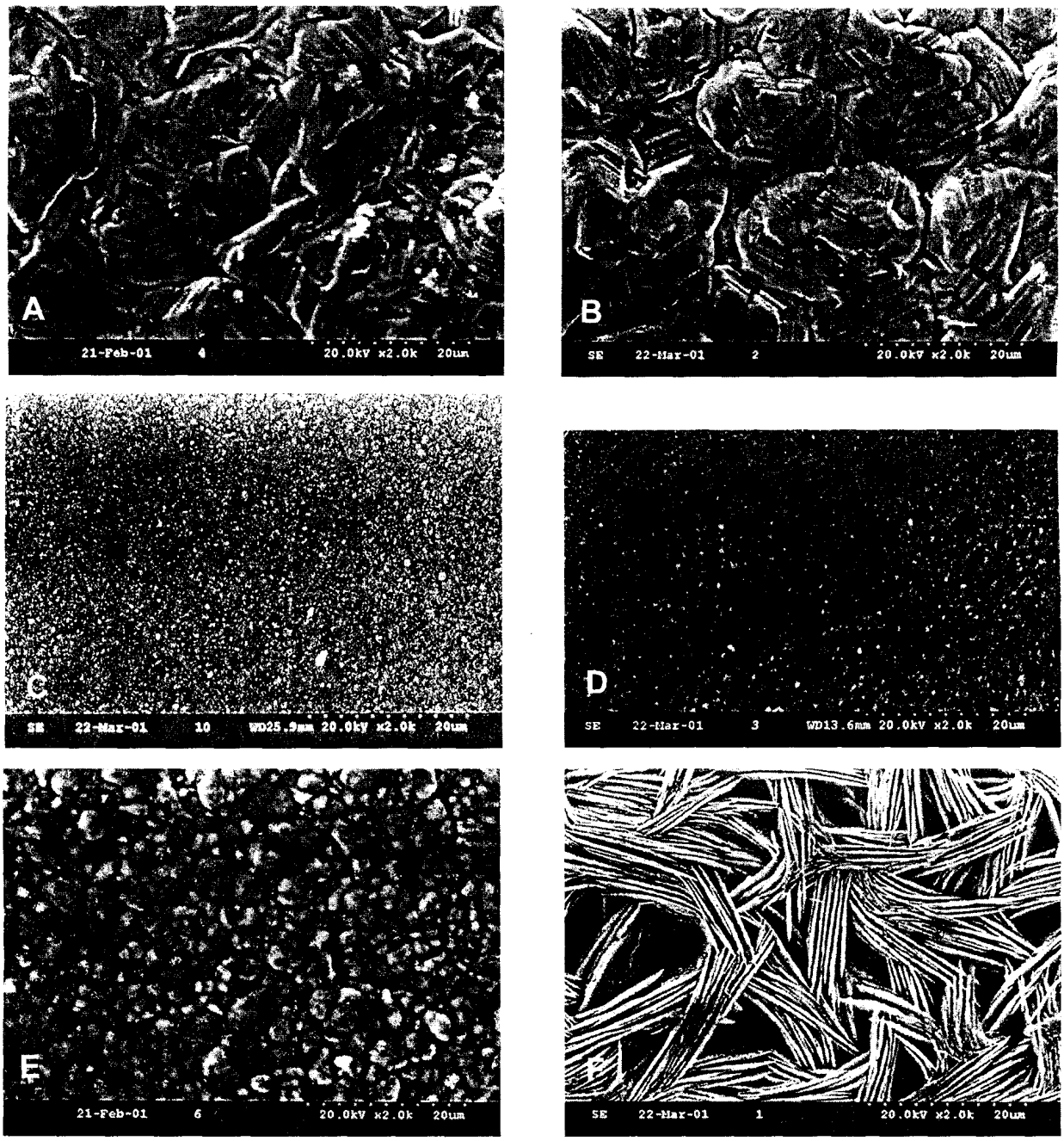

Figure 13—SEM photograph of zinc deposit obtained at (a) 30°C (86°F) from Bath A at 2.0 A/dm² (18.6 A/ft²); (b) 40°C (104°F) from Bath A at 2.0 A/dm² (18.6 A/ft²); (c) 30°C (86°F) from Bath B at 3.0 A/dm² (27.9 A/ft²); (d) 40°C (104°F) from Bath B at 3.0 A/dm² (27.9 A/ft²); (e) 30°C (86°F) from Bath C at 3.0 A/dm² (27.9 A/ft²) and (f) 40°C (104°F) from Bath C at 3.0 A/dm² (27.9 A/ft²).

Table 7
X-ray diffraction data for electrodeposited zinc obtained at 40°C (104°F)

Bath	'd' observed	'd' standard	hkl	Lattice parameters (nm)		c/a ratio	Structure
				a	c		
A	2.473 2.092 1.685 1.340 1.172 1.089	2.473 2.091 1.687 1.342 1.1729 1.090	002 101 102 103 112 104	2.6670	4.9326	1.8494	Hexagonal
B	2.479 2.319 2.097 1.335 1.173	2.473 2.308 2.091 1.332 1.1729	002 100 101 110 112	2.6777	5.0832	1.9125	Hexagonal
C	2.313 2.092	2.308 2.091	100 101	2.6706	4.9088	1.8380	Hexagonal

the (100) reflection plane was more predominant for the deposits obtained from thiamine hydrochloride and gelatin-containing baths. SEM studies show that fine grained deposits are obtained from baths containing the optimum concentration of thiamine hydrochloride and gelatin (3.0 g/L; 0.4 oz/gal) at 30°C (86°F). The following bath compositions and operating parameters are recommended for good quality industrial zinc plating:

Bath A

Zinc acetate	200 g/L (26.7 oz/gal)
Sodium acetate	100 g/L (13.3 oz/gal)
Aluminum sulfate	30 g/L (4.0 oz/gal)
Boric acid	60 g/L (8.0 oz/gal)
Current density	2.0 to 3.0 A/dm^2 (18.6 to 27.9 A/ft^2)
pH	5.0
Temperature	30°C (86°F)

Bath B

Zinc acetate	200 g/L (26.7 oz/gal)
Sodium acetate	100 g/L (13.3 oz/gal)
Aluminum sulfate	30 g/L (4.0 oz/gal)
Boric acid	60 g/L (8.0 oz/gal)
Thiamine hydrochloride	3.0 g/L (0.4 oz/gal)
Current density	2.5 to 5.0 A/dm^2 (23.2 to 46.5 A/ft^2)
pH	5.0
Temperature	30°C (86°F)

Bath C

Zinc acetate	200 g/L (26.7 oz/gal)
Sodium acetate	100 g/L (13.3 oz/gal)
Aluminum sulfate	30 g/L (4.0 oz/gal)
Boric acid	60 g/L (8.0 oz/gal)
Gelatin	3.0 g/L (0.4 oz/gal)
Current density	2.5 to 5.0 A/dm^2 (23.2 to 46.5 A/ft^2)
pH	5.0
Temperature	30°C (86°F)

References

1. E.B. Saubestre, J. Hajdu & J. Zehnder, *Plating*, **56**, 691 (1969).
2. W.E. Rosenberg & F.H. Holland, *Plating & Surface Finishing*, **78**, 51 (January 1991).
3. L. Grincevichene, R. Vishomirskis, S. Jakobson, B. Williams & T. Stasivk, *Metal Finishing*, **89**, 10 (July 1995).
4. S.M. Mayanna, T.V. Venkatesh, R.P. Dambal & J. Balachandra, *Metal Finishing*, **85**, 15 (July 1987).
5. T.V. Venkatesha, J. Balachandra, S.M. Mayanna & R.P. Dambal, *Plating & Surface Finishing*, **74**, 77 (June 1987).
6. T.V. Venkatesha, J. Balachandra, S.M. Mayanna & R.P. Dambal, *Metal Finishing*, **83**, 33 (August 1985).
7. M. Pushpavanam & B.A. Shenoi, *Metal Finishing*, **75**, 29 (January 1977).
8. S. Morisaki, T. Mori & S. Tajima, *Plating & Surface Finishing*, **68**, 55 (August 1981).
9. M. Chandran, R.L. Sarma & R.M..Krishnan, *Trans. IMF*, **81** 207 (2003).
10. H. Geduld (Ed), *Zinc Plating*, Finishing Publications, Teddington, UK (1988).
11. A. Ramachandran & S.M. Mayanna, *Metal Finishing*, **90**, 61 (February 1992).
12. P.J. Hancharik, *Plating & Surface Finishing*, **70**, 28 (November 1983).
13. S. Rajendran, S. Bharathi, C. Krishna & T. Vasudevan, *Plating & Surface Finishing*, **84**, 59 (March 1997).
14. R.M. Krishnan, S.R. Natarajan, V.S. Muralidharan & G. Singh, *Metal Finishing*, **89**, 15 (February 1991).
15. V. Ravindran, R.M. Krishnan & V.S. Muralidharan, *Metal Finishing*, **96**, 10 (October 1998).
16. V. Narasimhamurthy & B.S. Sheshadri, *Metal Finishing*, **96**, 24 (April 1998).
17. S.S. Abd El Rehim, S.M. Abd El Wahaab, E.E. Fouad & H.H. Hassan, *J. App. Electrochem.*, **24**, 350 (1994).

18. S.S. Abd El Rehim, E.E. Fouad, S.M. Abd El Wahaab & H.H. Hassan, *Electrochimica Acta*, **41**, 1413 (1996).
19. S.S. Abd El Rehim, M. Emad, M. Khaled, M. Fettonhi & J. Shirokoff, *Trans IMF*, **79**, 95 (2001).
20. E. Ranb & K Muller (Ed), *Fundamentals of Metal Deposition*, Elsevier, Amsterdam (1967).
21. V.S. Mohanty, B.C. Tripathy, P. Singh & S.C. Das, *J. Appl. Electrochem.*, **31**, 969 (2001).
22. P.A. Adcock, A. Quillinan, B. Clapk, O.M.G. Newman & S.B. Adeloju, *J. Appl. Electrochem.*, **34**, 771 (2004).
23. R. Sarmaitis, T. Bernatavicius, V. Dikinis, V. Rezaite & I. Demcenko, *Trans. IMF*, **81**, 19 (2003).
24. A. Narkevicius, D. Bucinskiene, M. Samuleviciene & R. Ramanauskas, Trans.IMF, **81**. 93 (2003).
25. D.S. Baik & D.J. Fray, *J. Appl. Electrochem.*, **31**. 1141 (2001).
26. K. Racissi, A. Saatchi & M.A.Golozar, *J. Appl. Electrochem.*, **33**, 635 (2003).

About the Authors

Dr. Ramachandran Sekar obtained his postgraduate degree in Chemistry in 1992 at Gandhigram Rural Institute (Deemed University), Gandhigram in Tamil Nadu, India. He is currently working at the Central Electrochemical Research Institute, Karaikudi, Tamil Nadu, India in the field of electroplating and industrial metal finishing. His fields of interest are eco-friendly non-cyanide zinc plating, cadmium plating, silver plating, nickel plating, chromium plating and gold plating. He has published 15 papers and holds two patents to his credit.

Dr. Sobha Jayakrishnan, M Sc., Ph.D is presently the Head of the Industrial Metal Finishing division of the Central Electrochemical Research Institute (CECRI), Karaikudi, India. She has been actively engaged in research work relating to electroplating of metals and alloys for the past 25 years.